



Jul 1st, 12:00 AM

Experimental and Computational Analysis of Microscale Wind Environmental Conditions in the Port of Rotterdam

Wendy Janssen

Bert Blocken

Herm Jan Van Wijhe

Follow this and additional works at: <https://scholarsarchive.byu.edu/iemssconference>

Janssen, Wendy; Blocken, Bert; and Van Wijhe, Herm Jan, "Experimental and Computational Analysis of Microscale Wind Environmental Conditions in the Port of Rotterdam" (2012). *International Congress on Environmental Modelling and Software*. 387. <https://scholarsarchive.byu.edu/iemssconference/2012/Stream-B/387>

This Event is brought to you for free and open access by the Civil and Environmental Engineering at BYU ScholarsArchive. It has been accepted for inclusion in International Congress on Environmental Modelling and Software by an authorized administrator of BYU ScholarsArchive. For more information, please contact scholarsarchive@byu.edu, ellen_amatangelo@byu.edu.

Experimental and Computational Analysis of Microscale Wind Environmental Conditions in the Port of Rotterdam

Wendy Janssen^a, Bert Blocken^a, Herm Jan van Wijhe^b

^a*Unit Building Physics and Services, Department of the Built Environment,
Eindhoven University of Technology, Eindhoven, The Netherlands*

^b*Port of Rotterdam, The Netherlands*

w.d.janssen@tue.nl

Abstract: Knowledge of microscale wind conditions is important for maneuvering and mooring of ships and for optimizing the harbor design. The aim of this study is to translate the macroscale wind conditions measured at a near shore reference station to the local (microscale) wind conditions in the harbor docks. In the first part of the project, an extensive experimental campaign has been performed, which consisted of wind velocity measurements with 2D and 3D ultrasonic anemometers during a period of 6 months. These point measurements confirm the unique relation between the macroscale and microscale wind conditions during periods of strong winds. As the measurements only provide information at a number of discrete positions, the second part of the study consists of numerical simulations with Computational Fluid Dynamics (CFD) to map the wind environmental conditions over the entire study area. The measurements and simulations both show very large gradients in mean wind speed over the harbor area, with differences up to 100%. The numerical simulations are currently in progress and will be validated by comparison with the on-site measurements.

Keywords: Computational Fluid Dynamics (CFD); wind environment; complex terrain; nautical aerodynamics.

1 INTRODUCTION

In the past decades, Computational Fluid Dynamics (CFD) has been developed and applied as a powerful tool for the assessment of microscale wind environmental conditions [Meroney 2004, Franke et al. 2007, Gromke et al. 2008, Tominaga et al. 2008, van Hooff and Blocken 2010, Tominaga and Stathopoulos 2010, Gousseau et al. 2011, Blocken et al. 2012]. CFD has some important advantages compared to wind tunnel testing. Wind tunnel measurements are generally only performed at a few selected points in the model area, and do not provide a whole image of the flow field. CFD on the other hand provides whole-flow field data, i.e. data on the relevant parameters in all points of the computational domain. Unlike wind tunnel testing, CFD does not suffer from violation of similarity requirements because simulations can be conducted at full scale. This is particularly important for extensive topographic areas such as the case study in this paper. However, the accuracy and reliability of CFD are important concerns. CFD verification and validation are imperative [e.g. Casey and Wintergerste 2000, Jakeman et al. 2006, Franke et al. 2007, Tominaga et al. 2008, Blocken et al. 2012, Blocken and Gualtieri 2012]. This requires experimental data, either wind tunnel data or field data. These data in turn need to satisfy certain quality criteria [Schatzmann et al. 1997, Schatzmann and Leitl 2011]. This paper presents the first results of an extensive case study in which a combination of on-site measurements and numerical simulations with CFD is applied to provide an accurate assessment

of the microscale wind conditions (mean wind speed, wind direction and turbulence intensities) over a large part of the harbor area of Rotterdam. The aim of the study is to provide wind velocity data that can be used as input for real-time maneuvering simulations to evaluate accessing the harbor with larger ships. A high-quality computational grid is made, and special care is given to the implementation of surface roughness parameterizations and the simulations are compared with on-site measurements. The present study focuses on high wind speed conditions, for which the atmospheric boundary layer exhibits neutral stratification. The reason is that high wind speeds are most relevant for maneuvering, due to the larger forces at higher wind speeds. In section 2, the geometry of the harbor area is briefly described. In section 3, the choice for CFD simulations over wind tunnel measurements in this study is clarified. Section 4 addresses the on-site measurements that have been made to validate the CFD simulations. In section 5, the computational settings and parameters for the CFD analyses are outlined, and some first results are presented.

2 GEOMETRY OF THE HARBOR AREA

The study focuses on the part of the harbor area shown in Figure 1, with indication of the names of the harbor docks. This area has a diameter of about 6.5 km, and it is characterized by constant changes in geometry. Large industrial objects are being built, landmass and harbor area is being added and finally ships may or may not be present at certain locations. These factors all have an influence on the microscale wind conditions. In addition, the roughness of the water surface (height of waves) is a function of the wind velocity.



Figure 1. Plan view of study area with names of main harbor docks and indication of the nine measurement positions.

3 WIND TUNNEL MODELING VERSUS CFD SIMULATION

The minimum horizontal distance that should be modeled is about 6 km (Figure 1). If the study of wind conditions would be performed in an atmospheric boundary layer wind tunnel, the reduced-scale model should therefore correspond to a full-scale situation of at least 6 km in diameter. Even for a large ABL wind tunnel with a test section of 3 m width, a scaling factor of at least 2000 would be required. For mean wind velocity at a height $H = 10$ m above mean sea level, the full-scale Reynolds number for a reference wind speed of $U_{10} = 10$ m/s is $Re = U_{10}H/\nu =$

6.8×10^6 , while the corresponding reduced-scale value would be $Re \approx 3400$, which is near the laminar regime. Clearly, no accurate results can be obtained with such a strong reduction in Reynolds number. At least equally important is the difficulty to perform near-ground measurements. A 1 mm hot sphere would already correspond to a 2 m object in full-scale, which will significantly affect the flow. Because wind tunnel modeling is not an option, numerical simulation with CFD is pursued to obtain realistic spatially and temporally varying wind velocity fields (mean wind speed, wind direction and turbulence intensity) over the harbor area. The simulations will be isothermal simulations with neutral atmospheric boundary layer approach-flow conditions, because the focus is on strong wind speed conditions, in which the mechanical production of atmospheric turbulence dominates over thermal effects. As mentioned earlier, validation of the numerical results by comparison with high-quality experiments is essential. Therefore, on-site measurements have been performed at nine selected positions.

4 ON-SITE MEASUREMENTS

On-site wind-velocity measurements with 3D and 2D ultrasonic anemometers were made at nine different positions from December 2010 – May 2011, with some minor interruptions in between. The criteria for selection of the measurement positions were: (1) representativeness for wind conditions in the harbor docks, therefore the positions are situated along the water front; (2) avoiding local disturbance effects by small-scale terrain features that are not included in detail in the numerical model, such as individual buildings and containers; and (3) safety and theft protection of the equipment. Position 1 (see Fig. 1) is the reference measurement position at which measurements are constantly performed by the Royal Dutch Meteorological Institute KNMI and passed on to the Harbor Authorities. It provides a good reference measurement position, because it is very exposed to the oncoming wind for almost all wind directions. The gathered field measurements were 1-minute data, which were converted (averaged) into 10-minute data to more strongly position them in the spectral gap of the wind speed power spectrum [van der Hoven 1957]. Only data for which the mean wind speed at the reference position is higher than 5 m/s were retained. This is important to exclude thermal effects from the comparison. As mentioned before, the simulations were performed for neutral atmospheric conditions, and thermal effects may be ignored. Around every of the 36 wind directions for which CFD simulations are being made ($0^\circ - 10^\circ - 20^\circ - 30^\circ - \dots - 350^\circ$), a relatively narrow 10° wind direction sector was defined. All experimental 10-minute data values that had 10-minute wind directions at point 1 within this sector, were attributed to this sector, after which averaged values and standard deviations were obtained. The comparison between the measurements at point 1 performed in the framework of this project and the measurements by the Harbor Authorities at almost the same position showed a very close agreement, with deviations in mean wind speed and mean wind direction generally less than 1%. For every measurement position and for each wind direction interval of 10° , the so-called amplification factor and the amplification vector were determined. The amplification factor at a measurement position is the ratio between the mean wind speed at that measurement position and the wind speed at the reference position. The amplification vector is the vector with the magnitude of the amplification factor and the direction of the local mean wind direction. In addition, the turbulence intensity was determined. For all 36 wind direction intervals, the amplification factors and the turbulence intensity have been averaged, and used to provide amplification vector maps, as shown in Figure 2. These maps also show the standard deviation of the wind direction by the two additional lines, symmetrical to the vector arrow itself. Figure 2 shows that the deviations in mean wind direction are rather small, but that the deviations in amplification factor (or mean wind speed) can be quite large. These observations are directly related to the different roughness of various parts of the terrain. In addition, also turbulence intensities and turbulence spectra were obtained (not shown here), which all provide valuable data for validation of the CFD simulations in a future stage of this project.

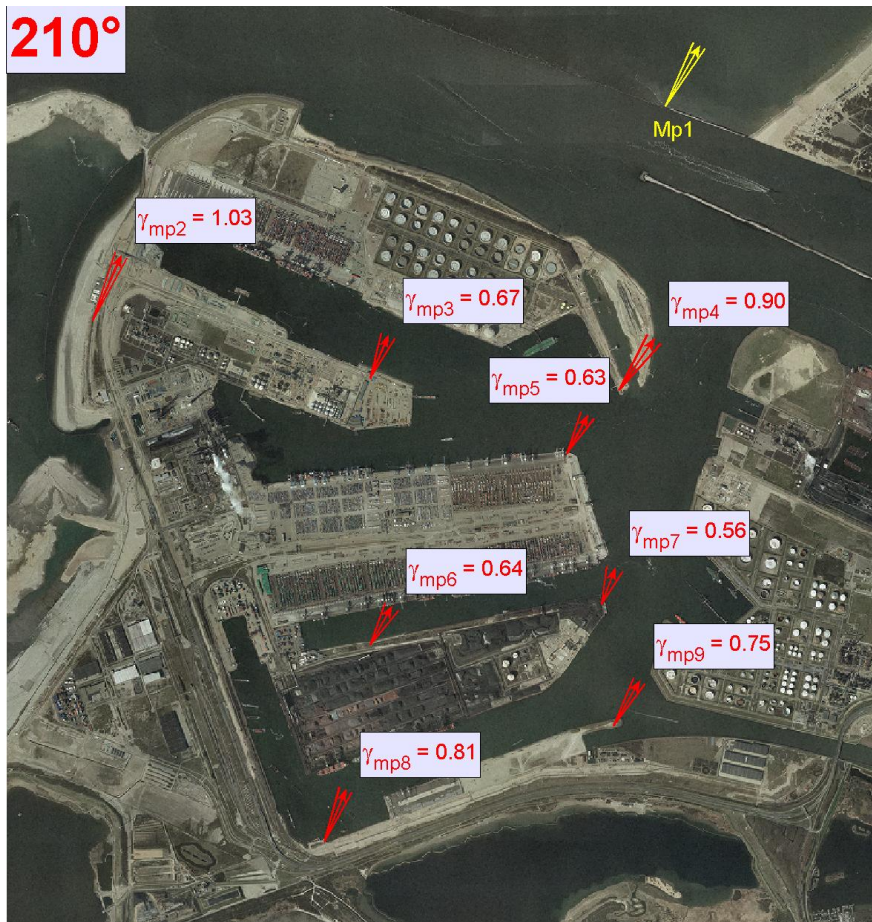


Figure 2. Amplification vectors and factors at the nine measurement positions for the prevailing wind direction 210°, indicating differences up to a factor 2 in mean wind speed.

5 CFD SIMULATIONS

5.1 Computational geometry and computational grid

The computational geometry is based on combination of GIS data, aerial photography, building plans and on-site visits (Figure 3 – left). The computational domain has dimensions length by width by height equal to 11750 x 11740 x 500 m³. The computational grid (Figure 3 – right) is generated using the surface extrusion grid technique presented by van Hooff and Blocken [2010]. This technique allows a large degree of control over the size and shape of the computational cells. It only uses hexahedral and prismatic cells, and no tetrahedral and pyramid cells. This reduces the numerical discretization error and allows the use of second-order discretization schemes without compromising convergence. This technique has been successfully applied in other studies to model complex urban areas [Gousseau et al. 2011, Blocken et al. 2012]. For the present simulation, the grid resolution in the vertical direction is 0.4 m for the first cell, and increases gradually with height until 36 m at the top of the domain. The resulting grid contains about 75 million control volumes. The computations are performed by parallel processing on twelve HP DL360R07 Xeon X5650 2.66 GHz processors with 96 Gb RAM.

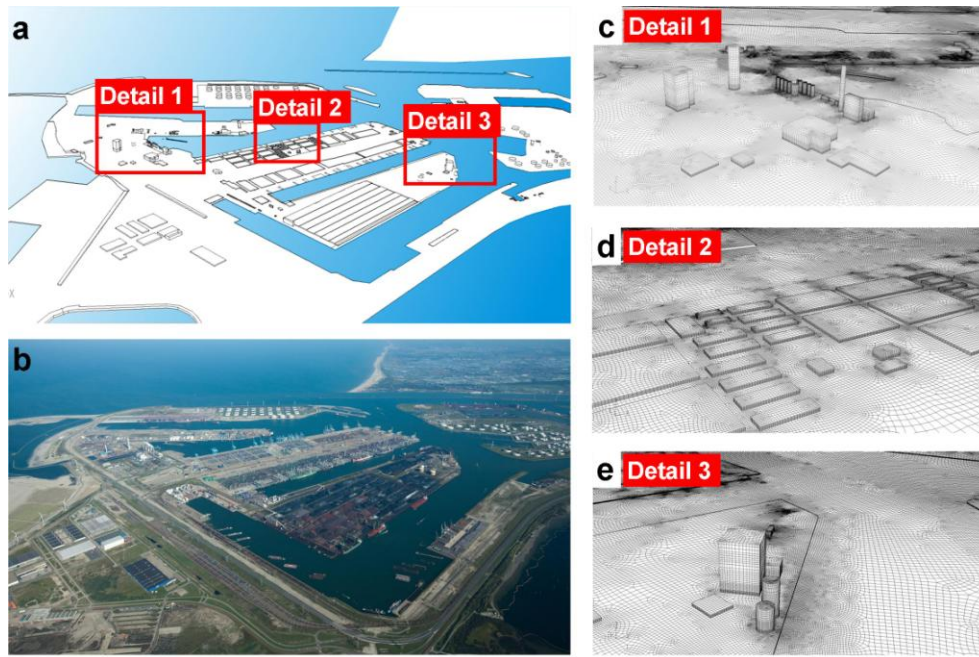


Figure 3. Left: CFD model geometry and corresponding photograph. Right: Selected parts of the computational grid.

5.2 Boundary conditions and solver settings

A distinction is made between two types of roughness [Blocken et al. 2007]: (1) the roughness of the terrain that is included in the computational domain and (2) the roughness of the terrain that is not included in the computational domain. The knowledge of the roughness of the terrain that is situated outside the computational domain is important because it determines the shape of the inlet profiles of mean wind speed and turbulence. These profiles are generally expressed as a function of the aerodynamic roughness length z_0 [Wieringa 1992]. This parameter can be determined based on a roughness estimation of the terrain that extends from the inlet of the computational domain up to about 5-10 km from this inlet. This assessment is performed using the roughness classification of Davenport, updated by Wieringa [1992]. On the other hand, the roughness of the terrain inside the computational domain is important because it determines to a large extent the local flow conditions and the development of internal boundary layers in the domain. For CFD codes that use wall functions with a roughness modification based on the equivalent sand-grain roughness height k_s and the roughness constant C_s , such as the code Fluent 6.3 [Fluent 2006] used in this study, three steps are required: (1) subdivision of the terrain into patches with similar roughness; (2) estimation of the local z_0 using the roughness classification [Wieringa 1992]; and (3) conversion of z_0 into the corresponding wall function parameters k_s and C_s . This is performed using the appropriate conversion equation, which, for Fluent 6.3, was derived by Blocken et al. [2007]:

$$k_{s,ABL} = \frac{9.793 z_0}{C_s} \quad (1)$$

At the inlet of the domain, the profiles of mean wind speed U , turbulent kinetic energy k and turbulence dissipation rate ε are based on the estimated z_0 of the upstream terrain, using the equations by Richards and Hoxey [1993]:

$$U(z) = \frac{u_{ABL}^*}{\kappa} \ln\left(\frac{z + z_0}{z_0}\right) \quad (2)$$

$$k(z) = \frac{u_{ABL}^{*2}}{\sqrt{C_\mu}} \quad (3)$$

$$\varepsilon(z) = \frac{u_{ABL}^{*3}}{\kappa (z + z_0)} \quad (4)$$

where u_{ABL}^* is the ABL friction velocity, κ the von Karman constant (0.42) and C_μ a constant equal to 0.09. Note that these profiles are different for different wind directions, due to the variation of z_0 with wind direction. For the ground surface, the standard wall functions by Launder and Spalding [1974] with roughness modification by Cebeci and Bradshaw [1977] and the appropriate parameters k_s and C_s are applied. The sides and top of the domain are modeled as a slip walls (zero normal velocity and zero normal gradients of all variables). At the outlet, zero static pressure is set. The 3D Reynolds-Averaged Navier-Stokes (RANS) equations are solved with the commercial CFD code Fluent 6.3 [Fluent Inc. 2006] using the control volume method. The realizable k- ε model [Shih et al. 1995] is used to provide closure. Second-order discretization schemes are used for both the convective and viscous terms of the governing equations. The SIMPLE algorithm is used for pressure-velocity coupling and standard pressure interpolation is used. Calculations are performed for 36 wind directions: $0^\circ - 10^\circ - \dots - 350^\circ$. Convergence is assumed to be obtained when all the scaled residuals [Fluent Inc. 2006] have leveled off.

5.3 First results

The CFD simulations are currently ongoing. Some first results are shown in Figure 4. This figure shows wind speed contours over part of the harbor area, at a height of 7 m above MSL, for reference wind speed of 5 m/s and reference wind direction 210° . The simulation results confirm the strong variation of wind speed conditions over the area. Further simulations and a detailed comparison between CFD results and on-site measurements are currently being performed.

6 SUMMARY AND CONCLUSIONS

This paper has presented an experimental analysis and the first results of a numerical analysis of microscale wind conditions for the Port of Rotterdam. This information is important for maneuvering and mooring of ships and for optimizing the harbor design. The aim of this study is to translate the macroscale wind conditions measured at a near shore reference station to the local (microscale) wind conditions in the harbor docks. First, an extensive experimental campaign was performed, which consisted of wind velocity measurements with 2D and 3D ultrasonic anemometers during a period of 6 months. These point measurements confirmed the unique relation between the macroscale and microscale wind conditions during periods of strong winds. As the measurements only provide information at a number of discrete positions, the second part of the study consisted of numerical simulations with Computational Fluid Dynamics (CFD) to map the wind environmental conditions over the entire study area. The measurements and simulations both show very large gradients in mean wind speed over the harbor area, with differences up to 100% at relatively "open" or exposed conditions, confirming the complexity of the wind environmental conditions and the necessity of their assessment for improving harbor operations. The numerical simulations are currently ongoing and will be validated by comparison with the on-site measurements.

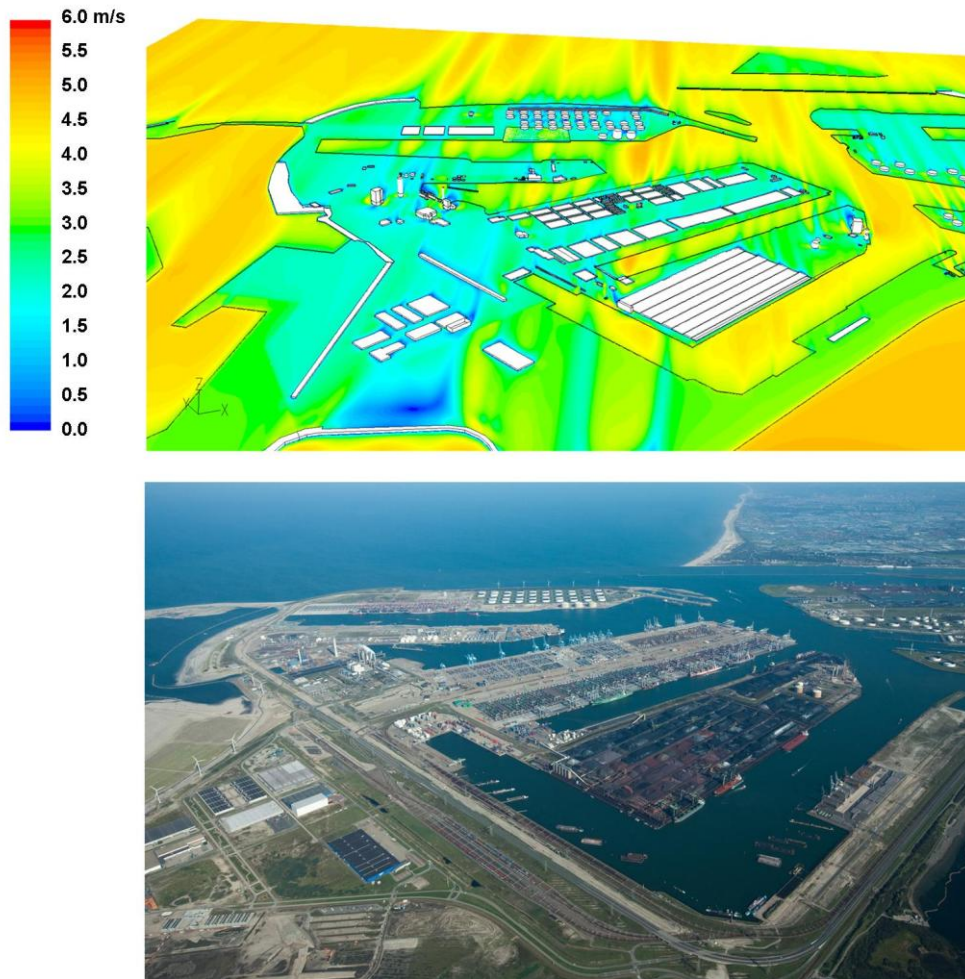


Figure 4. Top: Contours of wind speed at a height of 7 m above MSL, for reference wind speed of 5 m/s and wind direction 210°. Bottom: Corresponding aerial photograph.

REFERENCES

- Blocken, B., T. Stathopoulos, and J. Carmeliet, CFD simulation of the atmospheric boundary layer: wall function problems, *Atmospheric Environment*, 41(2), 238-252, 2007.
- Blocken, B., and C. Gualtieri, Ten iterative steps for model development and evaluation applied to Computational Fluid Dynamics for Environmental Fluid Mechanics, *Environmental Modelling & Software*, 33, 1-22, 2012.
- Blocken, B., W.D. Janssen, and T. van Hooff, CFD simulation for pedestrian wind comfort and wind safety in urban areas: General decision framework and case study for the Eindhoven University campus, *Environmental Modelling & Software*, 30, 15-34, 2012.
- Casey, M., and T. Wintergerste, *Best Practice Guidelines*, ERCOFTAC Special Interest Group on Quality and Trust in Industrial CFD, ERCOFTAC, Brussels, 2000.
- Cebeci, T., and P. Bradshaw, *Momentum transfer in boundary layers*, Hemisphere Publishing Corporation, New York, 1977.
- Fluent Inc., *Fluent 6.3 User's Guide*. Fluent Inc., Lebanon, 2006.
- Franke, J., A. Hellsten, H. Schlünzen, and B. Carissimo, *Best practice guideline for the CFD simulation of flows in the urban environment*, COST 732: Quality Assurance and Improvement of Microscale Meteorological Models, 2007.

- Gromke, C., R. Buccolieri, S. Di Sabatino, and B. Ruck, Dispersion study in a street canyon with tree planting by means of wind tunnel and numerical investigations - Evaluation of CFD data with experimental data, *Atmospheric Environment*, 42(37), 8640-8650, 2008.
- Jakeman, A.J., R.A. Letcher, and J.P. Norton, Ten iterative steps in development and evaluation of environmental models. *Environmental Modelling & Software*, 21(5), 602-614, 2006.
- Lauder, B.E., and D.B. Spalding, The numerical computation of turbulent flows. *Computer Methods in Applied Mechanics and Engineering*, 3, 269-289, 1974.
- Meroney, R.N., *Wind tunnel and numerical simulation of pollution dispersion: a hybrid approach*, Working paper, Croucher Advanced Study Institute on Wind Tunnel Modeling, Hong Kong University of Science and Technology, 6–10 December, 2004.
- Ramponi, R., and B. Blocken, CFD simulation of cross-ventilation for a generic isolated building: impact of computational parameters, *Building and Environment*, 53, 34-48, 2012.
- Richards, P.J. and R.P. Hoxey, Appropriate boundary conditions for computational wind engineering models using the k- ϵ turbulence model, *Journal of Wind Engineering and Industrial Aerodynamics*, 46&47, 145-153, 1993.
- Schatzmann, M., and B. Leidl, Issues with validation of urban flow and dispersion CFD models. *Journal of Wind Engineering and Industrial Aerodynamics*, 99(4), 169-186, 2011.
- Schatzmann, M., S. Rafailidis, and M. Pavageau, Some remarks on the validation of small-scale dispersion models with field and laboratory data, *Journal of Wind Engineering and Industrial Aerodynamics* 67&68, 885-893, 1997.
- Shih, T.H., J. Zhu, and J.L. Lumley, A new Reynolds stress algebraic equation model, *Computer Methods in Applied Mechanics and Engineering*, 125, 287–302, 1995.
- Tominaga, Y., A. Mochida, R. Yoshie, H. Kataoka, T. Nozu, M. Yoshikawa, and T. Shirasawa, AIJ guidelines for practical applications of CFD to pedestrian wind environment around buildings, *Journal of Wind Engineering and Industrial Aerodynamics* 96(10-11), 1749-1761, 2008.
- Tominaga, Y., Stathopoulos, T., 2010. Numerical simulation of dispersion around an isolated cubic building: Model evaluation of RANS and LES. *Build. Environ.* 45(10), 2231-2239.
- Van der Hoven, I., Power spectrum of horizontal wind speed in the frequency range from 0.0007–900 cycles per hour, *Journal of Meteorology* 14, 160–164, 1957.
- van Hooff, T. and B. Blocken, B., Coupled urban wind flow and indoor natural ventilation modelling on a high-resolution grid: A case study for the Amsterdam ArenA stadium, *Environmental Modelling & Software*, 25(1), 51-65, 2010.
- Wieringa, J., Updating the Davenport roughness classification, *Journal of Wind Engineering and Industrial Aerodynamics*, 41-44, 357-368, 1992.